Visualization of Flow Separation around an Atmospheric Entry Capsule at Low-Subsonic Mach Number using Background-Oriented Schlieren (BOS)

Toshiharu Mizukaki[1]
Tokai University, Hiratsuka,Kanagawa, Japan, 259-1292

Stephen E. Borg, Paul M. Danehy[2]
Advanced Sensing and Optical Measurement Branch
NASA Langley Research Center, Hampton, VA, 23681-2199

and

Scott M. Murman
Fundamental Modeling & Simulation Branch
NASA Ames Research Center, Moffett Field, CA, 94035

This paper presents the results of visualization of separated flow around a generic entry capsule that resembles the Apollo Command Module (CM) and the Orion Multi-Purpose Crew Vehicle (MPCV). The model was tested at flow speeds up to Mach 0.4 at a single angle of attack of 28 degrees. For manned spacecraft using capsule-shaped vehicles, certain flight operations such as emergency abort maneuvers soon after launch and flight just prior to parachute deployment during the final stages of entry, the command module may fly at low Mach number. Under these flow conditions, the separated flow generated from the heat-shield surface on both windward and leeward sides of the capsule dominates the wake flow downstream of the capsule. In this paper, flow visualization of the separated flow was conducted using the background-oriented schlieren (BOS) method, which has the capability of visualizing significantly separated wake flows without the particle seeding required by other techniques. Experimental results herein show that BOS has detection capability of density changes on the order of 10^{-5}.

I. Introduction

The design and analysis of Earth-entry capsules, such as the Orion Multi-purpose Crew Vehicle, poses a challenge in the subsonic regime due to the three-dimensional separation and unsteady wake flow encountered. Unfortunately, this is often where greatest accuracy is required, as there is little margin in control authority and complex parachute decelerator staging must be accomplished for targeted landing. In order to improve our engineering capability, a better understanding of the fluid mechanics of these configurations is required, notably at the high Reynolds number conditions encountered in flight. Recently, experimental Particle-Image Velocimetry (PIV) and Schlieren measurements of a simplified Orion capsule shear layer and wake were obtained.[1] The current work complements these approaches using a simple, economical Schlieren method, which has the potential to provide both qualitative and accurate quantitative data for capsule shear layers and wake flows.

II. Background-Oriented Schlieren (BOS)

Background-Oriented Schliern (BOS) has been proposed and used to visualize the flow density change for one decade.[2-15] Its principle of operation is relatively simple and the method is easy to carry out with a commercial-off-the-shelf apparatus. The BOS method can provide quantitative flow visualization images with relatively simple

[1] Professor, Department of Aeronautics and Astronautics, 4-1, Kitakaname, Senior member AIAA.
[2] Research Scientist, MS 493, Associate Fellow AIAA.

optics (consisting of a few commercial off-the-shelf components) while not requiring a laser. From an optics viewpoint, the BOS method is a white light speckle photography method that is similar to the laser-speckle method, except that a white light source is used to record instead of a laser. However, from the image-processing viewpoint, the BOS method uses a method similar to particle image velocimetry (PIV). A significant difference between BOS and PIV is that PIV uses micro-particles, such as oil mist or dust in the air, to detect flow. Conversely, the BOS method uses the background pattern (including random dots) located on the opposite side of the test section from the camera. Density variations in the air cause the background pattern to distort, allowing the density variations to be measured.

In 1998,[15] Meier proposed a visualization technique that can provide density distribution inside fluid phenomenon of interest by detecting and analyzing the distribution of the background-pattern displacement using digital image processing. The method is named the background-oriented schlieren (BOS) method or background-oriented optical tomography (BOOT). The principal advantage of this technique, in comparison with other density-recording optical techniques such as the shadowgraph, schlieren, speckle, and interferometry methods, is its extremely modest equipment requirements The technique usually only requires one (electronic) camera, a sufficiently structured background, a light source, and a personal computer (PC). The reason this technique has not been widely applied until now is probably because of the requirement for fast and accurate de-convolution algorithms, which have only recently become available for PCs.

Another advantage of the BOS method is its theoretically unlimited field of view, which means its capacity to monitor objects of unlimited size. Because of the conical viewing field of the camera used, the size of a subject is usually restricted by its distance from, and the focal length of, the imaging lens employed. However, the conical shape of the projection and different sensitivities of the spatially distributed schlieren necessitate certain correction and calibration procedures. An additional difficulty is the need to focus the background and the object simultaneously. This configuration is achieved by using a sufficiently small aperture: large F-number, to keep both within the depth of field (DOF) or using telecentric optics. Generally speaking, the sensitivity of BOS increases with increasing the distance ratio $e = Z_D/Z_B$ (see Fig. 1) while large e needs long DOF which is difficult to set up in a small laboratory. The optimal sensitivity and resolution of the setup are achieved when the background structure has a texture close to, but slightly larger than, the camera resolution.

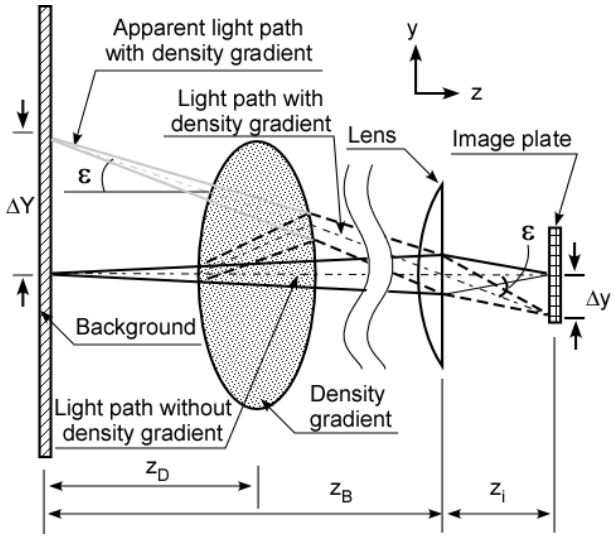

Figure 1. Principle of Background-Oriented Schlieren.

Since the refraction of a single beam contains information about the spatial gradient of the refractive index integrated along the axial path, the image refraction angle in radians, ε, is defined as[13]:

$$\varepsilon = \frac{1}{n_0}\int_{Z_D-\Delta Z_D}^{Z_D+\Delta Z_D}\frac{\delta n}{\delta y}dZ \tag{1}$$

with the assumption that ΔZ_D, the half-width of the region of the density gradient, is $\Delta Z_D << Z_D$. Further, it is seen from the geometry (see Fig. 1) that the virtual image displacement is related to the image displacement by the lens distance from the background Z_B and the image distance from the lens Z_i , which, for large Z_B, can be replaced by

the focal length f of the lens:

$$\frac{\Delta Y}{Z_B} = \frac{\Delta y}{Z_i} = \frac{\Delta y}{f} \tag{2}$$

For small deflection angles, ε can be approximated as

$$\Delta y = Z_D M \, \varepsilon \tag{3}$$

where $M = Z_i / Z_B = f / Z_B$. Hence,

$$\varepsilon = \frac{Z_B \Delta y}{Z_D f} \tag{4}$$

The magnitude of the background displacement on the image obtained of the shear layer was provided by an image-matching algorithm based on the cross-correlation function between the target image and the reference image. The refraction angle, ε, of the light passing through phenomenon of interest, is then determined by equation (3). The relationship between density and the index of refraction is described as Gladstone-Dale formula,

$$n - 1 = K\rho, \tag{5}$$

where K is Gradstone-Dale constant, and ρ is density of medium. Therefore, once Δy is revealed, one can estimate the density of the subject.

III. Experimental Method

A. One-dimensional density distribution measurement

The first aim of this one-dimensional BOS measurement is to verify applicability of BOS measurements on density distribution for subsonic flows ranging up to Mach 0.40. An additional goal of the present research is to quantitatively detect the weak density disturbance caused by the shear layer around the capsule model in subsonic flows. Theoretically, BOS allows one to obtain quantitative information on density gradients in any type of flow provided that a proper distance between the test section and the background is available for sufficient image shift on the surface of the imaging device, such as a CCD camera. However, generally speaking, the limitations of the size of a measurement area in a wind tunnel facility gives a maximum distance from the test section to the background pattern. In the present case, available distance from background pattern to camera through the test section of our wind tunnel is about two meters at a maximum.

The second aim of the one-dimensional BOS measurement is to verify the effect on background displacement by varying the focal length of the imaging lens, the distance ratio from the test section to the background versus the imaging lens to the background, and the depth of field. Equations (3) and (4) suggest that the larger distance, Z_D, produces a larger displacement on the surface of the imaging device, and that the longer focal length of the imaging lens the higher the sensitivity. In the present study, sub-pixel precision is needed to visualize the shear layer clearly. Reliability of the equations remains unclear for small density gradients with maximum displacement of background images with sub-pixel order.

Figure 2 shows the experimental apparatus for validation of the accuracy of a one-dimensional BOS measurement. A one-dimensional density distribution is generated in a closed-glass-walled vessel with 500-mm depth, 300-mm width, and 270-mm height, which is equipped with heated and cooled top and bottom walls. The ceiling, equipped with a 20-W-sheet heater and the bottom surface attached with a water-bath filled with circulated-low-temperature water at 0 degrees, induced a temperature gradient in the air inside the vessel. The air temperature inside the vessel was recorded by ten type-K thermocouples on a wooden plate at intervals of 25.4 mm. The thermocouple output is accurate to 0.05 K and has a temporal interval of temperature measurements of 0.5 sec, and is recorded by a data logger. The background pattern used here was a random-dot pattern, which was printed on normal printing paper and illuminated from its backside with a halogen lamp. A CMOS camera (4096 by 3072 pixel, 6 um x 6 um for one element size, Teledyne Dalsa Falcon2) with a 50-mm-focal-length lens was used to record images of the background through the vessel; one image for reference and another after the temperature distribution. The F-number used here was F/22 to create enough depth of field (DOF) to record the phenomena inside the vessel and the background pattern on the imaging plane simultaneously. The distances between the background to the imaging lens, Z_B, and to the center of the vessel, Z_D, were 4.75 meters and 2.45 meters, respectively. The heater started heating the air in the vessel from the ceiling and the cold water circulation cooled from the bottom after recording a non-disturbed reference image of the background. One hundred images were recorded with 20 ms exposure times and a 0.5 Hz of frame interval, after establishing a stable temperature distribution. During the

recording, the temperature indicated by the thermocouples near the top and the bottom of the chamber were 26.0 and 16.0 degrees Celsius, respectively. Background displacement on each image was calculated with the cross-correlation function from which large noise and error which were exceeded the certain value based on the standard deviation of all the displacements were removed. For the calculation, the minimum interrogation window size was eight by eight pixels. The overlapping ratio of the interrogation window was 0.875 and the processed displacement with coordinate information was temporally and spatially averaged.

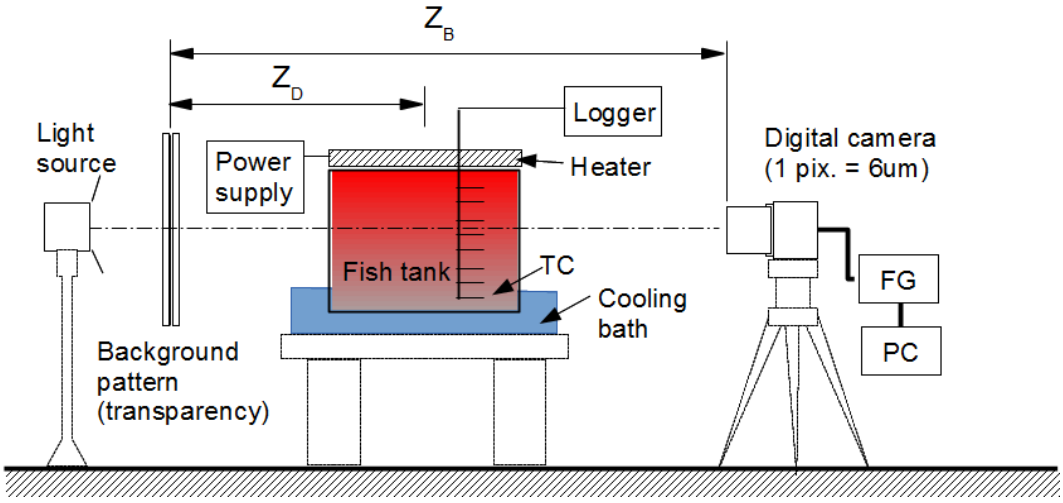

Figure 2. Setup for one-dimensional density gradient measurement by BOS.

Figure 3 shows the results of the displacement calculation of the background through the vessel along the distance from the surface of the ceiling, which was kept heated by a sheet-type heater. Figure 3a shows the temperature distribution in the vessel. Open circles indicate temperature of the air at each thermocouple and the red-solid line represents the temperature gradient indicated by K/mm and is based on the measured temperature. Figure 3b shows color map of background displacement. Green indicates zero-pixel shift and red indicates +0.5-pixels shift which means an upward shift of 0.5-pixels. Figure 3c shows a comparison of the displacement of the background between BOS measurements and theoretical estimation based on the measured temperature. Open circles indicate the background displacement, which was determined by the cross-correlation function with the reference image, and the red-solid line is the temperature gradient distribution measured with thermocouples. Near the ceiling region the temperature gradient induced the pattern displacement with about 0.3-pixels, which was larger than the other region because the temperature dropped rapidly with the increasing distance from the ceiling. At the mid-region of the vessel, displacement decreased to less than 0.1 pixels because the temperature gradient decreased to about -0.03 K/mm. Near the bottom region, temperature gradient slightly decreased, again, because of the cooled bottom. As shown in Fig. 3c, BOS precisely detected sub-pixel displacement induced by the temperature gradient in the air.

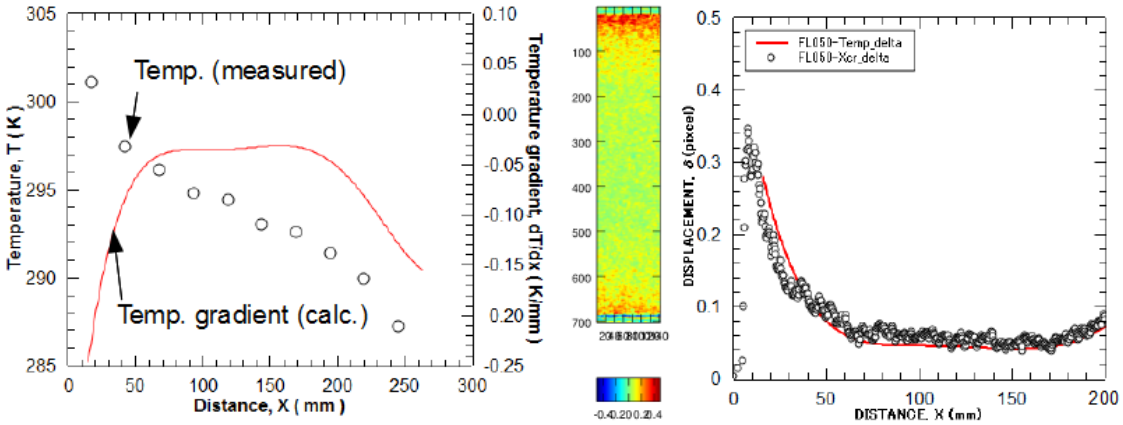

(a) Temperature profile (b) Map of displacement (c) Profile of displacement

Figure 3. Results of one-dimensional density distribution measurement.

Figure 4 shows displacement of the background, δ, through the vessel along the distance from the ceiling surface. An imaging lens with a focal length of 35 mm was used with an F-number of F/22. The distance from the background to the center of the vessel Z_D was 0.75 m, while the distance to the imaging lens Z_B was varied at 1.50 m, 2.25 m, and 3.75 m. Those values provide 0.50, 0.33, and 0.20 of distance ratio e (Z_D/Z_B). As shown in Figs.4a, 4b, and 4c, each result of three measurement's varying e suggests that equations (3) and (4) are still reliable even for applying for sub-pixel measurement. The difference among each result is sensitivity of BOS. In this experiment, loss of sensitivity of the BOS system appears as fluctuations (noise) in the displacement. As shown in the figures, fluctuations of displacement increases with increasing of distance ratio e. Figure 4a shows relatively large fluctuations of background displacement δ while other two do not. Then, small value of the distance ratio e allows to avoid noisy images, especially for need of detecting sub-pixel displacement.

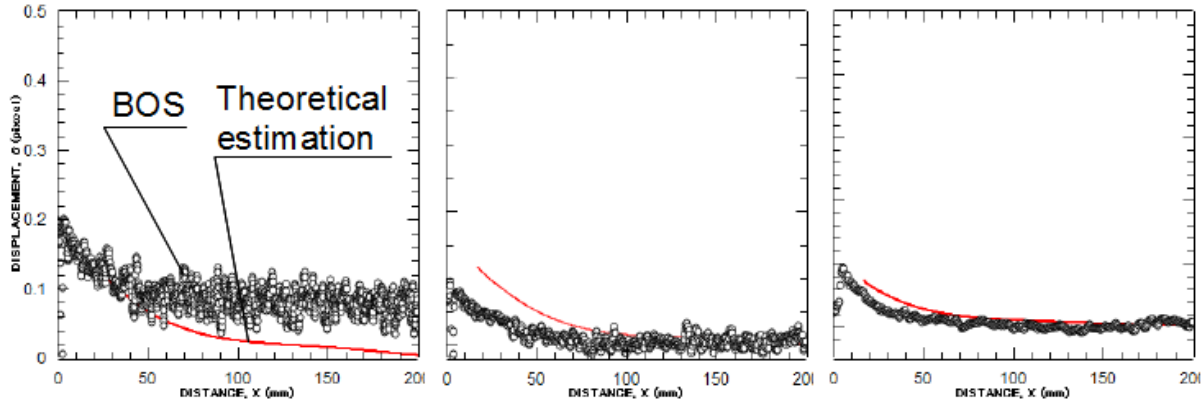

(a) Z_B =1.50 m (e = 0.50) (b) Z_B =2.25 m (e = 0.33) (c) Z_B = 3.75 m (e = 0.20)

Figure 4. Comparisons of background displacement between BOS measurement and theoretical estimation based on temperature gradients taken by same focal length f = 35 mm with different distance ratios e.

B. Subsonic Wind Tunnel Experiment

A capsule model mounted on a sting with an angle of attack at 28 degrees was studied. Figure 5 shows some of the dimensions of the 4" (101.6 mm) diameter model. The model was installed with the sting horizontal in the test section of the subsonic wind tunnel. The wind tunnel has a nearly octagonal cross section with an inner diameter of approximately 13". Velocities of the main flow were measured with a pitot probe and converted to Mach number. Conditions with Mach 0.1, 0.2, 0.3, 0.35, and 0.4 were used.

Figure 6 shows the experimental setup. A random-dot pattern where the diameter and ratio of the black area to the white one was 0.20 mm and 20%, respectively, was used as background. Reference images, wind-off images, and test images (wind-on) were recorded with the same industrial video camera for one-dimensional density measurements, Teledyne Dalsa Falcon 2. Flow field images were recorded for one second at a framing rate of 50 Hz and an exposure time of 20 ms for each shot. The oscillation frequency of fluid phenomena is characterized by the Strouhal number St,= $f D/U$ where f, D, and U represent the frequency of the oscillation, the characteristic length, and the velocity of the fluid, respectively. In the present case, under the assumption that the capsule model is a sphere with 100-mm diameter in Mach 0.40 flow, St, D, and U are 0.2,[16] 136 m/s, and 0.1 m, respectively. The frequency of wake turbulence behind the capsule f was estimated to be about 270 Hz. Therefore, the exposure time to freeze the oscillation of the wake needed to be from two to three milliseconds. However, in the present paper, attempts to obtaining frozen images of the wake were not made because of weak light intensity of the images (which could be improved in future experiments). Background displacement caused by the flow around the model was determined by a cross-correlation analysis with the reference image. In this experiment, the distances from the background to the center of the wind tunnel, Z_B, and to the camera lens, Z_D, were 150 mm and 835 mm. The focal length of the camera lens was 100 mm, and F-number F/22 was chosen.

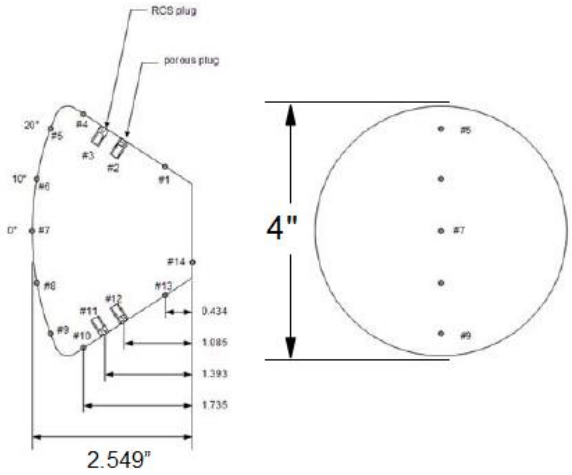

(a) Side view (b) Bottom (Heat shield) –side surface

Figure 5. The generic entry capsule model examined in 13" subsonic wind tunnel.

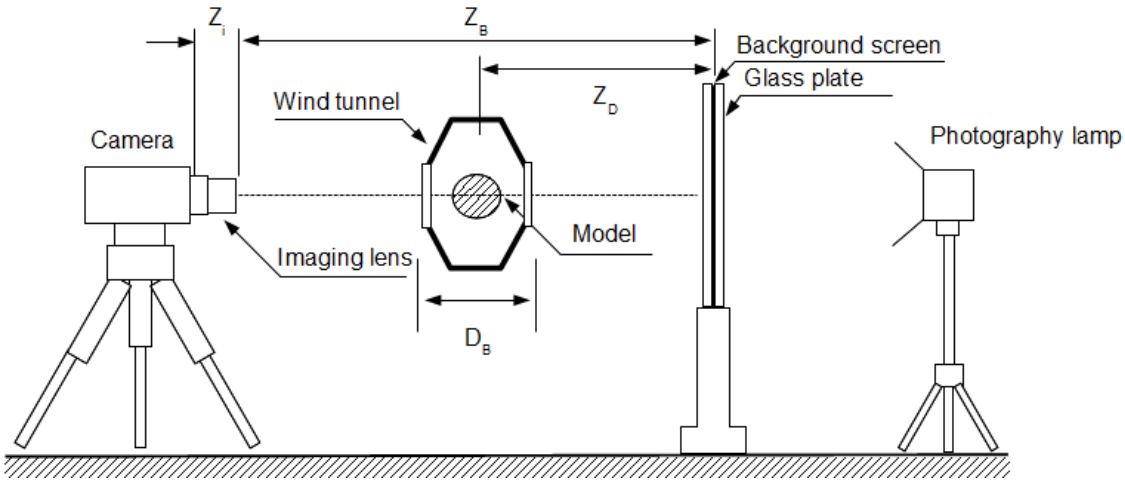

Figure 6. Schematic diagram of visualization setup of BOS for 13" subsonic wind tunnel.

IV. Computational Method

Reynolds-averaged Navier-Stokes (RANS) simulations using Menter's Shear-Stress-Transport (SST) model were computed with the OVERFLOW2 solver. The overset grid system for the capsule alone contains 17M grid points. The computational approach has been validated as part of the Orion program by detailed comparisons against wind tunnel data for surface static and unsteady pressures, along with off-body Particle Image Velocimetry (PIV) measurements of the separating shear-layer and wake.

V. Experimental and Computational Results

Figure 7 shows maps of background displacement induced by the flow around the capsule model at flow Mach number 0.1, 0.2, 0.3, 0.35, and 0.4. Upper row represents horizontal displacement toward the right-hand-side and the lower row shows vertical displacement. The colors in the figures indicate background displacement in pixels ranging from -0.5 (blue) to +0.5 (red). In this experiment, negative values of displacement indicate a positive density gradient. On both displacement maps the shear layer, which was emerging from the shoulder of the heat-shield and the side surface of the capsule model toward the downstream, clearly appears in flows with velocity faster than M = 0.3. Also, in front of the capsule model, the expansion region, where the flow was accelerated while turning around the shoulder from the heat shield to the main flow, clearly appears. The strength of the expansion region gradually increased in both directions. In Fig. 7, the thickness of the shear layer does not represent the actual thickness because of integrated displacement along the line of sight. The actual shear layer around the capsule model is expected to have oscillation and curvature so that the visualized image shows a thicker shear layer in Fig. 7. Generally speaking, at lower Mach number, the oscillation amplitude should be larger than that at higher Mach

number because of the decreasing oscillation frequency as Mach number increases. Therefore, the shear layer in Fig. 7c has a weaker and broader appearance than that in Figs. 7d and e. There is a difference in background color across the upper row of Fig. 7b and c. Theoretically, there should be no displacement in the main flow which would have uniform density distribution. Curiously, the background shift has appeared mainly in the x-direction. Nonetheless, the cause for this small sub-pixel shift remained unexplained.

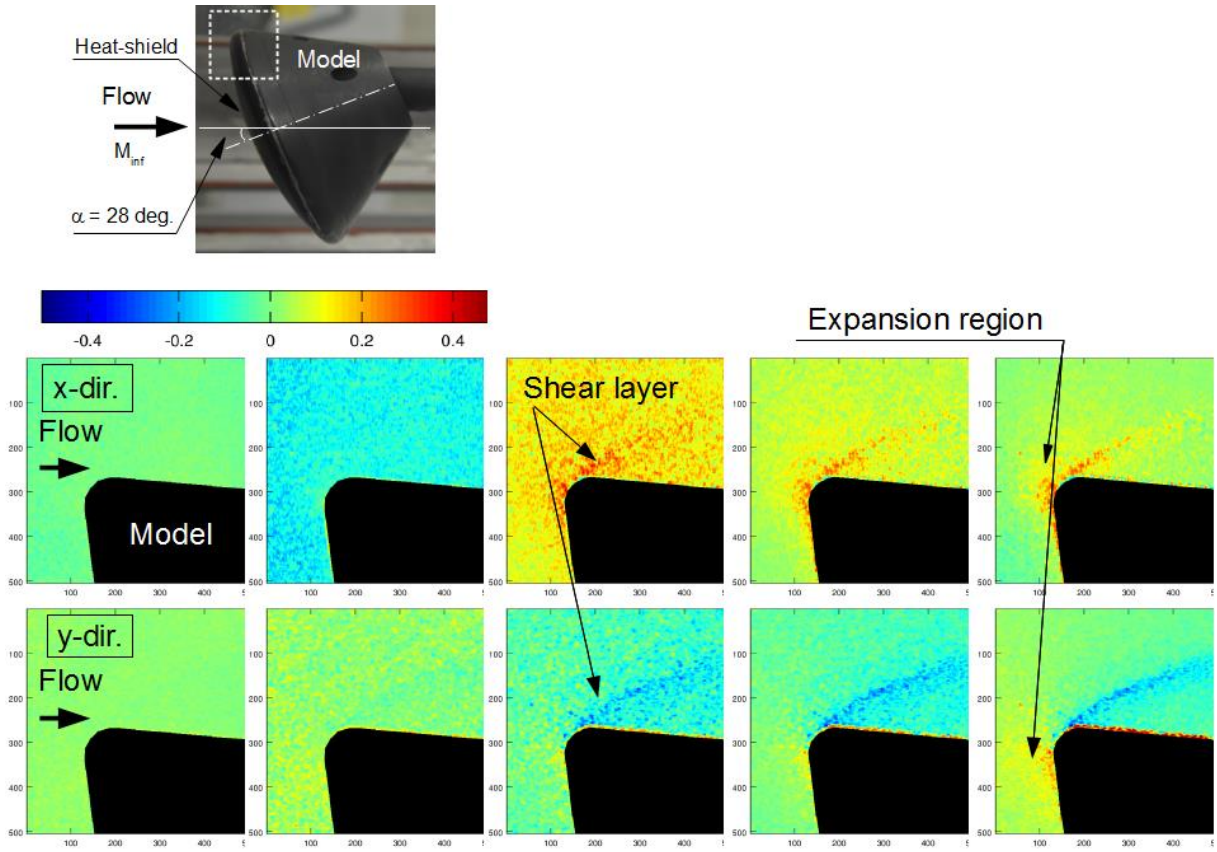

(a) M0.10 (b) M 0.20 (c) M0.30 (d) M0.35 (e) M0.40

Figure 7. Maps of background displacement on flow Mach numbers ranging from 0.1 to 0.4.

Under the assumption of two-dimensional flow on the examined flow field, the relative-density difference that was induced by the flow around the capsule model was estimated. Figure 8 shows a horizontal and vertical density change profile across the flow around the capsule model at Mach number 0.4. Figures 8b and 8c show the relative-density-difference profile based on displacement of the background along the broken line X-X' and Y-Y' in Fig. 8a. Black dots indicate the density profile determined as a percentage of atmospheric density of the day of the measurement, 1.258 kg/m^3. The origin of broken lines is at the left-end and the top for X-X' and Y-Y', respectively. Figure 8b shows that a density decrease of about 0.04% from main flow was induced across the shear layer emanating from the shoulder. Figure 8c shows that, in the expansion region in front of the capsule model, a density decrease of about 0.04% was induced.

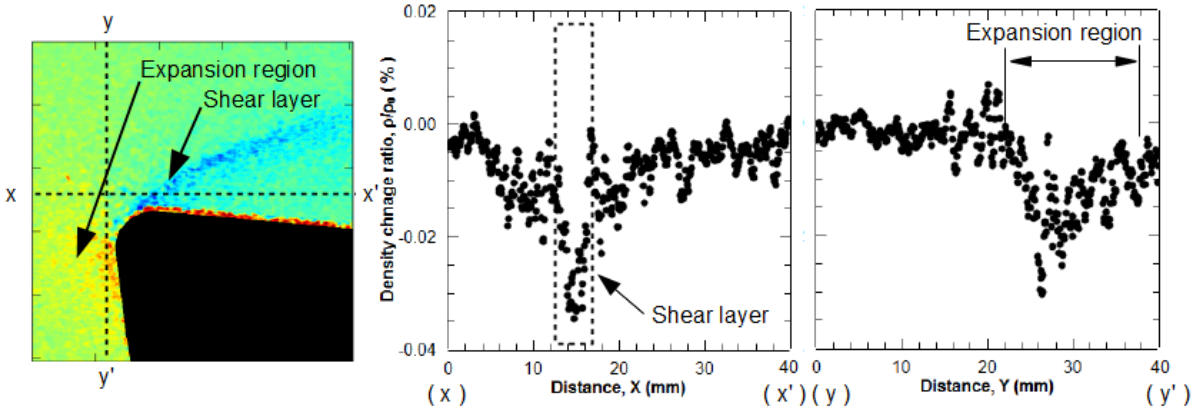

(a) Examined lines (b) Along the line X-X' (c) Along the line Y-Y'

Figure 8. Density profile across the flow field.

Figure 9 shows the density field around the capsule model from the CFD simulation, along with two BOS windows superimposed on the image. The contour lines represent the computed result and the pixel pattern the BOS results. In region "A", the shear layer separating from near the maximum diameter of the capsule is clearly visualized by the BOS technique, and matches quite well qualitatively with the computational result. Similarly, a small expansion region just upstream of the separation is captured, which also agrees with the computational result. In region "B", the large expansion region developing in front of the heat shield, is clearly visualized with color contour. The shear layer emanating from the marginal region of the heat shield and the side surface is also captured well.

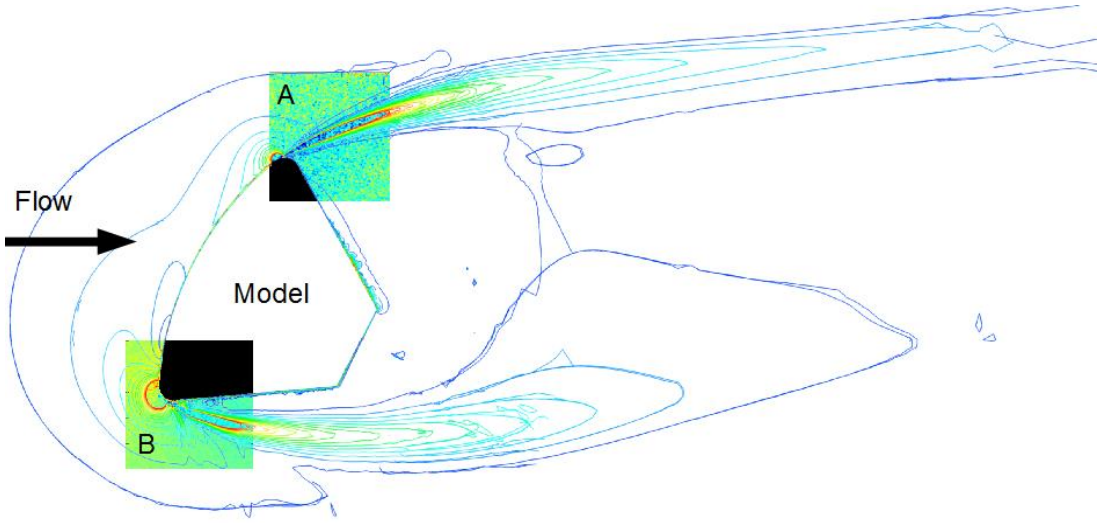

(a)

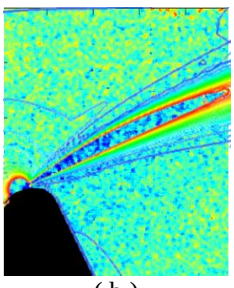

(b)

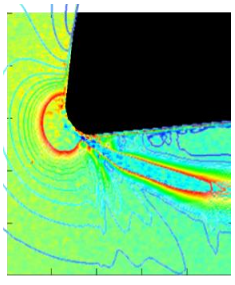

(c)

Figure 9. Comparison of BOS result with numerical result around the model. a, Superimposed BOS results on the computational result (Global flow field); the BOS results represent background displacement while the computational result density ; **b**, magnification of Region "A"; **c**, magnification of Region "B".

VI. Summary

The background-oriented schlieren (BOS) method was used to visualize the separated flow on the wake of a capsule entry vehicle at low subsonic speed at a fixed angle of attack of 28 degrees. The flow field around the capsule model was examined in the test section of a subsonic wind tunnel with flow speed ranging from Mach 0.1 to 0.4. Both the shear layer emanating from edge of the model and the expansion region in front of the capsule model were clearly visualized by BOS and agreed qualitatively well with a computational simulation. This experimental result suggests that BOS with a fine-pixel imaging device has detection capability of 10^{-5}-order-density-changing in subsonic flow. This result shows that BOS has the capability of qualitative, and potentially quantitative, visualization for complicated subsonic flows without the need for particle seeding, toxic gas seeding, or complicated and expensive laser technology.

References

[1] Ross, J. C., Heineck, J. T., Burnside, N., Sellers, M. E., Halcomb, N., Garbeff, T., Yamauchi, G., and Kushner, L. "Comprehensive Study of the Flow Around a Simplified Orion Capsule Model," *31st AIAA Applied Aerodynamics Conference*. American Institute of Aeronautics and Astronautics, 2013.

[2] Mizukaki, T., Matsumura, T., Wakabayashi, K., and Nakayama, Y. "Background-oriented schlieren with natural background for quantitative visualization of open-air explosions," *Shock Waves* Vol. 24, No. 1, 2014, pp. 69-78.

[3] Schairer, E., Kushner, L., and Heineck, J. "Measurements of tip vortices from a full-scale UH-60A rotor by retro-reflective background oriented schlieren and stereo photogrammetry," *69th American Helicopter Society Annual Forum*. Phoenix, AZ, 2013, p. Paper #403.

[4] Bauknecht, A., Merz, C., Landolt, A., Meier, A., and Raffel, M. "Blade tip vortex detection in maneuvering flight using the Background Oriented Schlieren (BOS) technique," *69th American Helicopter Society Annual Forum*. Phoenix, AZ, 2013, p. #145.

[5] Venkatakrishnan, L. "Density field measurements of a supersonic impinging jet with microjet control," *AIAA Journal* Vol. 49, No. 2, 2011, pp. 432-437.

[6] Krimse, T., Agocs, J., Schröder, A., Schramm, J. M., Karl, S., and Hannemann, K. "Application of particle image velocimetry and the background-oriented schlieren technique in the high-enthalpy shock tunnel Göttingen," *Shock Waves* Vol. 21, 2011, pp. 233-241.

[7] Mizukaki, T. "Visualization of compressible vortex rings using the background-oriented schlieren method," *Shock Waves* Vol. 20, 2010, pp. 531-537.

[8] Leopold, F. "The application of the colored background oriented schlieren technique (CBOS) to wind tunnel, free-flight and in-flight measurements," *Journal of Flow Visualization and Image Processing* Vol. 16, No. 4, 2009, pp. 279-293.

[9] Hargather, M. J., and Settles, G. S. "Natural-background-oriented schlieren imaging," *Experiments in Fluids* Vol. 48, No. 1, 2009, pp. 59-68.

[10] Sommersel, O. K., Bjerketvedt, D., Christensen, S. O., Krest, O., and Vagsaether, K. "Application of background oriented schlieren for quantitative measurements of shock waves from explosions," *Shock Waves* Vol. 18, No. 4, 2008, pp. 291-297.

[11] Venkatakrishnan, L. "Density measurements in an axisymmetric underexpanded jet by background-oriented schlieren technique," *AIAA Journal* Vol. 43, No. 7, 2005, pp. 1574-1579.

[12] Venkatakrishnan, L., and Meier, G. E. A. "Density measurements using the Background Oriented Schlieren technique," *Experiments in Fluids* Vol. 37, No. 2, 2004, pp. 237-247.

[13] Meier, G. E. A. "Computerized background-oriented schlieren," *Experiments in Fluids* Vol. 33, No. 1, 2002, pp. 181-187.

[14] Richard, H., and Raffel, M. "Principle and applications of the background oriented schlieren (BOS) method," *Measurement Science and Technology* Vol. 12, No. 9, 2001, pp. 1576-1585.

[15] Meier, G. E. A. "New optical tools for fluid mechanics," *8th International Symposium on Flow Visualization*. Sorrento, 1998, p. Paper 226.

[16] Sakamoto, H., and Haniu, H. "A Study on Vortex Shedding From Spheres in a Uniform Flow," *Journal of Fluids Engineering* Vol. 112, No. 4, 1990, pp. 386-392.